

Alex Tapper

Imperial College London

The Blackett Laboratory, Prince Consort Road, London SW7 2BW, United Kingdom

Measurements of the cross sections for charged and neutral current deep inelastic scattering at HERA are presented. The proton structure functions  $F_2$ ,  $F_L$  and  $xF_3$  are extracted from the measured neutral current cross sections and found to be in agreement with the Standard Model expectations. The measured cross sections are used as input to next-to-leading order QCD analyses to extract the parton distribution functions in the proton.

## 1. Introduction

Deep inelastic scattering (DIS) of leptons off nucleons probes the structure of matter at small distance scales. Two types of DIS interactions are possible at HERA: neutral current (NC) reactions  $e^-p \rightarrow e^-X$  and  $e^+p \rightarrow e^+X$ , where a photon or  $Z^0$  boson is exchanged and charged current (CC) interactions  $e^-p \rightarrow \nu X$  and  $e^+p \rightarrow \bar{\nu}X$ , where a  $W^\pm$  boson is exchanged.

The HERA accelerator collides electrons or positrons with protons. In the years 1994 to 2000 the H1 and ZEUS detectors collected positron-proton data samples of approximately  $100 \text{ pb}^{-1}$  each and electron-proton data samples of around  $16 \text{ pb}^{-1}$  each. Until 1998 HERA collided positrons or electrons of energy 27.6 GeV with 820 GeV protons, yielding collisions at a centre-of-mass energy of  $\sim 300 \text{ GeV}$ . For the 1998 running period the proton beam energy was increased to 920 GeV, increasing the centre-of-mass energy to  $\sim 320 \text{ GeV}$ .

The kinematics of charged current and neutral current deep inelastic scattering processes are defined by the four-momenta of the incoming lepton ( $k$ ), the incoming proton ( $P$ ), the outgoing lepton ( $k'$ ) and the hadronic final state ( $P'$ ). The four-momentum transfer between the electron and the proton is given by  $q = k - k' = P' - P$ . The square of the centre of mass energy is given by  $s = (k + P)^2$ . The description of DIS is usually given in terms of three Lorentz invariant quantities, which may be defined in terms of the four-momenta  $k$ ,  $P$  and  $q$ :

- $Q^2 = -q^2$ , the negative square of the four-momentum transfer,

- $x = \frac{Q^2}{2P \cdot q}$ , the Bjorken scaling variable,
- $y = \frac{q \cdot P}{k \cdot P}$ , the fraction of the energy transferred to the proton in its rest frame.

These variables are related by  $Q^2 = xys$ , when the masses of the incoming particles can be neglected.

Measurements of the neutral and charged current deep inelastic scattering cross sections as functions of  $x$  and  $Q^2$  and the proton structure functions extracted from these measurements are presented. Next-to-leading order QCD analyses of the measured cross sections within the framework of the Standard Model yield the parton distribution functions (PDFs) of the proton.

## 2. Experimental setup

The ZEUS and H1 detectors are described in detail elsewhere [1, 2]. The measurements presented make use primarily of the calorimeters, tracking detectors and luminosity measurement detectors. Selection of neutral current DIS events is based on the identification of a scattered electron or positron. The primary signature of charged current DIS events is missing transverse momentum from the final-state neutrino, which escapes undetected.

## 3. Cross sections

The double-differential Born-level cross section for the neutral current deep inelastic scattering processes  $e^-p \rightarrow e^-X$  and  $e^+p \rightarrow e^+X$ , with longitudinally unpolarised beams, is given by:

$$\frac{d^2\sigma_{\text{Born}}(e^\pm p)}{dx dQ^2} = \frac{2\pi\alpha^2}{xQ^4} [Y_+ F_2(x, Q^2) - y^2 F_L(x, Q^2) \mp Y_- x F_3(x, Q^2)], \quad (1)$$

where  $Y_\pm = 1 \pm (1 - y)^2$ , and  $\alpha$  is the QED coupling constant. The neutral current structure functions in the quark parton model are given by:

<sup>†</sup>Presented at New Trends in High-Energy Physics, Alushta, Crimea, Ukraine, May 24-31, 2003

$$F_2(x, Q^2) = \frac{1}{2} \sum_q [(V_q^L)^2 + (V_q^R)^2 + (A_q^L)^2 + (A_q^R)^2] [xq(x, Q^2) + x\bar{q}(x, Q^2)],$$

$$xF_3(x, Q^2) = \sum_q [V_q^L A_q^L - V_q^R A_q^R] [xq(x, Q^2) - x\bar{q}(x, Q^2)],$$

where the sums run over all quarks,  $q$ , in the proton. In the quark parton model  $F_L$  is zero. At next-to-leading order in QCD however quarks interact through gluons, which can split to quark-antiquark pairs or gluon pairs. In this way the struck quarks can have transverse momentum leading to a non-zero contribution from  $F_L$ . Thus,  $F_L$  is a direct probe of the gluon density in the proton. The structure function  $xF_3$  has contributions from the interference between the photon and  $Z^0$  exchange amplitudes, and pure  $Z^0$  exchange. The functions  $V_q$  and  $A_q$  contain the couplings of the electron to the photon and  $Z^0$ . The NC reduced cross section,  $\tilde{\sigma}_{NC}$ , is defined to be:

$$\tilde{\sigma}_{NC}(x, Q^2) = \frac{1}{Y_+} \frac{xQ^4}{2\pi\alpha^2} \frac{d^2\sigma_{Born}^{NC}}{dx dQ^2}.$$

The double-differential Born-level cross section for the longitudinally unpolarised charged current deep inelastic scattering processes  $e^-p \rightarrow \nu X$  and  $e^+p \rightarrow \bar{\nu} X$  are given by:

$$\frac{d^2\sigma_{Born}^{CC}(e^-p)}{dx dQ^2} = \frac{G_F^2}{2\pi} \frac{M_W^4}{(Q^2 + M_W^2)^2} \times [(u+c) + (1-y)^2(\bar{d} + \bar{s})], \quad (2)$$

$$\frac{d^2\sigma_{Born}^{CC}(e^+p)}{dx dQ^2} = \frac{G_F^2}{2\pi} \frac{M_W^4}{(Q^2 + M_W^2)^2} \times [(\bar{u} + \bar{c}) + (1-y)^2(d + s)], \quad (3)$$

where for example the PDF  $d$  is the density of down quarks in the proton at a given  $x$  and  $Q^2$ .  $M_W$  is the mass of the  $W$  boson and  $G_F$  is the Fermi constant. The CC reduced cross section,  $\tilde{\sigma}_{CC}$ , is given by:

$$\tilde{\sigma}_{CC} = \frac{2\pi}{G_F^2} \left( \frac{Q^2 + M_W^2}{M_W^2} \right)^2 \frac{d^2\sigma_{Born}^{CC}}{dx dQ^2}.$$

#### 4. Extraction of the proton structure functions

The NC cross section is dominated by the structure function  $F_2$  over most of the kinematic range. Thus,  $F_2^{em}$ , the purely electromagnetic part of  $F_2$ , may be extracted in the kinematic region where contributions from  $F_L$  and  $xF_3$  are small from the measured cross section by calculating correction factors for the effects of  $Z^0$  exchange in  $F_2$  and  $xF_3$  and the longitudinal structure function  $F_L$  and applying these to the measured cross section.

In order to extract the longitudinal structure function,  $F_L$ , the shape of the cross section as a function of  $y$  is used. The H1 and ZEUS collaborations have developed different techniques for the extraction of  $F_L$ . The latest method used by the H1 collaboration [3] makes use of a fit to the reduced cross section of the form:

$$\sigma_{FIT} = c \cdot x^{-\lambda} - \frac{y^2}{1 + (1-y)^2} F_L,$$

where  $c$ ,  $\lambda$  and  $F_L$  are free parameters and the first term describes  $F_2$ . The fit is performed as a function of  $x$  at fixed values of  $Q^2$ . The ZEUS collaboration make use of NC DIS events in which a hard initial state photon is detected at a small angle in the calorimeter of the luminosity monitor [4]. This effectively lowers the centre-of-mass energy of the collision which means that for a given  $x$  and  $Q^2$  there is a range of  $y$  values accessible. Exploiting the shape of the cross section as a function of  $y$  it is possible to extract  $F_L$  by fitting the following form to the ratio of data events to simulated events:

$$\frac{N_{DATA}}{N_{MC}(F_L = 0)} = N \cdot \frac{F_2 - (1-\epsilon)F_L}{F_2},$$

where  $N$  and  $F_L$  are free parameters,  $\epsilon = \frac{2(1-y)}{1+(1-y)^2}$  and  $F_2$  is measured in the same kinematic region using the procedure described above.

It can be seen from Eqn. (1) that the structure function  $xF_3$  can be extracted by subtracting the reduced cross section for positron-proton scattering from that for electron-proton scattering.

#### 5. QCD analysis

The measured cross sections have been used by both the H1 and ZEUS collaborations as input to QCD analyses in order to extract information on the parton density functions. The DGLAP evolution equations are used to predict the  $Q^2$  dependence of the PDFs, but experimental data must be used to constrain the  $x$  dependence of the input distributions at some starting scale,  $Q_0$ . Two complementary fits from H1 and ZEUS are presented.

The ZEUS-S fit [5] includes data from fixed-target experiments in order to constrain the fit in kinematic regions where the ZEUS NC data [6] are not sensitive. The starting scale  $Q_0^2=7 \text{ GeV}^2$  is chosen and the Thorne-Roberts variable flavour number scheme [7] is used to treat the heavy quarks. In contrast the H1 PDF 2000 fit [8] uses only data from the H1 collaboration to constrain the PDFs. NC and CC DIS measurements at high  $Q^2$  are used to constrain the valence quark distributions resulting in uncertainties within a factor of two compared to the fixed-target constraints used in the ZEUS fit. The starting scale  $Q_0^2=4 \text{ GeV}^2$  is chosen and a zero mass variable flavour number scheme is used for the treatment of the heavy quarks. In the absence of deuteron data from HERA the sea-quark and antiquark distributions are assumed to be equal. Both fits include careful treatment of the point-to-point correlated uncertainties in the data sets.

## 6. Results and interpretation

The electromagnetic part of the structure function  $F_2$  is shown in Fig. 1. Measurements from the H1 [8, 9, 10, 11] and ZEUS [6] collaborations are shown along with results from fixed-target experiments. It can be seen that the measurements span values of  $Q^2$  from  $1 \text{ GeV}^2$  up to  $30000 \text{ GeV}^2$ , and values of  $x$  from  $0.00006$  to  $0.65$ . The precision of the measurements is limited to 2-3% by systematic uncertainties below  $Q^2$  values of approximately  $1000 \text{ GeV}^2$  and by statistical uncertainties at higher values of  $Q^2$ . The Standard Model (SM) evaluated with PDFs from the H1 and ZEUS fits [8, 5] gives an excellent description of the data over the entire range of the measurements.

A summary of all H1 data on  $F_L$  is shown in Fig. 2. The data points range from  $Q^2$  of  $0.75 \text{ GeV}^2$  to  $700 \text{ GeV}^2$  for fixed  $W$  (photon-proton centre-of-mass energy) of  $276 \text{ GeV}$ . The data consist of the preliminary results described above and results based on earlier data, analysed with a slightly different procedure [8]. The SM predictions from the H1, ZEUS, MRST(2001) [12] and Alekhin [13] QCD fits are shown. All fits describe the data well at higher  $Q^2$ . The data do not favour the small values of  $F_L$  predicted by the MRST(2001) and ZEUS fits at low  $Q^2$ .

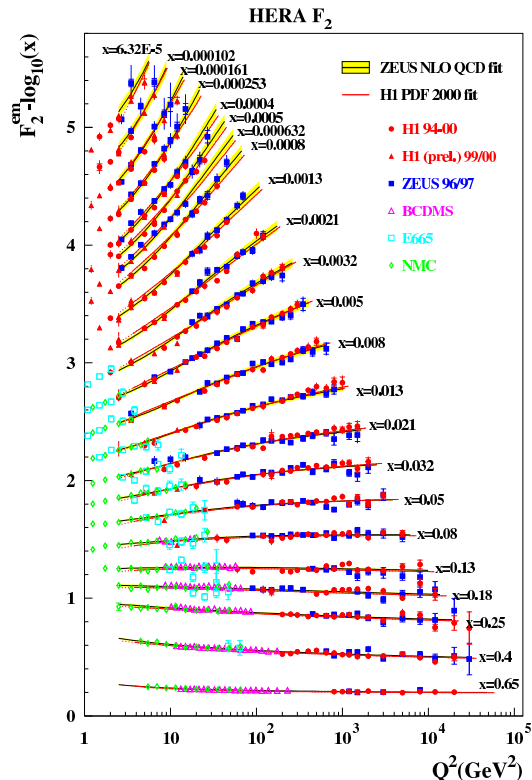


Fig. 1:  $F_2^{em}$  measured by the H1 and ZEUS collaborations.

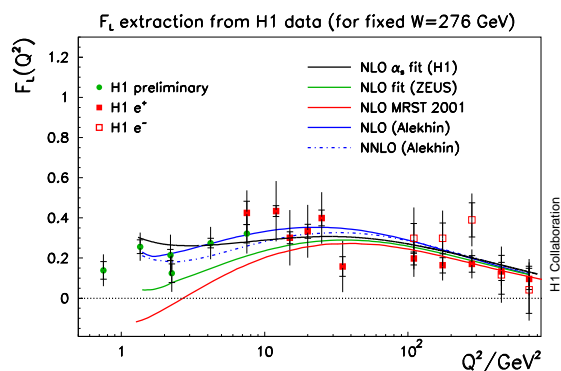


Fig. 2:  $F_L$  values from the H1 collaboration.

Figure 3 shows the value of  $F_L$  determined by the ZEUS collaboration. It is compared to the predictions for  $F_2$  and  $F_L$  from the ZEUS NLO QCD fit. The measurement is clearly consistent with the expectations of perturbative QCD. A more precise direct measurement of  $F_L$  could be made by varying the proton beam energy.

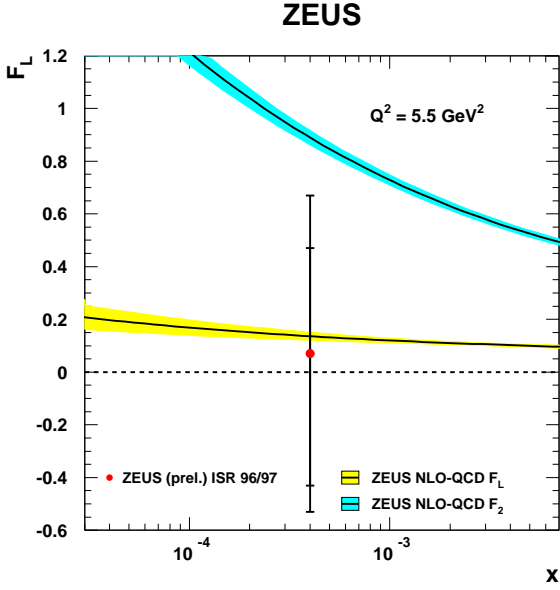


Fig. 3:  $F_L$  from the ZEUS collaboration.

Figure 4 shows the reduced NC cross sections for  $e^+p$  and  $e^-p$  scattering, measured by the H1 collaboration [8, 14].

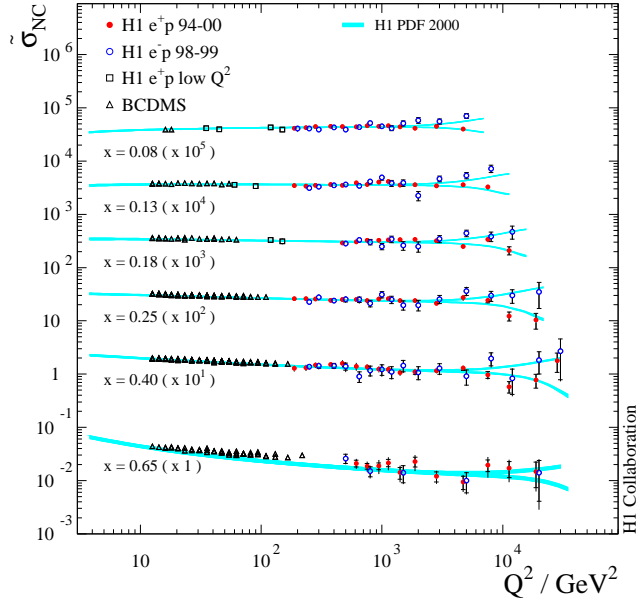


Fig. 4: The reduced cross section for NC DIS from the H1 collaboration.

The cross sections are plotted at fixed values of  $x$  as

functions of  $Q^2$ , and are well described by the Standard Model evaluated with the H1 2000 PDF fit. At the higher end of the  $Q^2$  range it can be seen that the cross section for  $e^-p$  scattering is higher than that for  $e^+p$ . The Standard Model predicts a higher cross section for  $e^-p$  interactions, due to constructive interference between the photon and  $Z^0$  exchange amplitudes, compared to  $e^+p$  interactions where destructive interference is expected.

The NC cross sections for  $e^-p$  and  $e^+p$  scattering can be subtracted to extract the structure function  $xF_3$ . Figure 5 shows the structure function  $xF_3$  extracted by the ZEUS [15] and H1[8] collaborations. Both are shown at fixed values of  $Q^2$  as functions of  $x$ , and are found to be well described by the Standard Model prediction evaluated using the CTEQ6D [16] PDFs. The data confirm the valence structure of the proton at high  $Q^2$ .

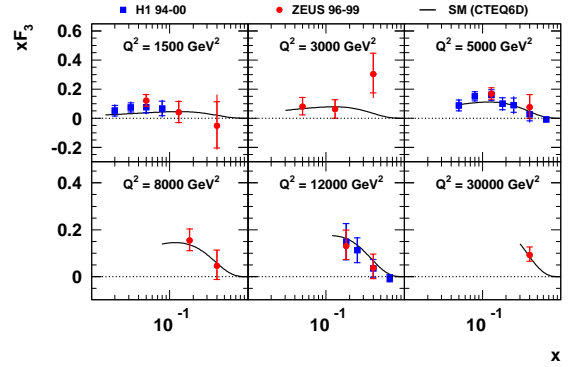


Fig. 5: The  $xF_3$  structure function from the H1 and ZEUS collaborations.

Figure 6 shows the reduced cross section for charged current  $e^+p$  interactions at fixed values of  $Q^2$  as a function of  $x$  measured by the H1 collaboration [8]. It can be seen from Eqn. (3) that  $e^+p$  CC DIS at high  $x$  and high  $Q^2$  probes the  $d$ -quark density. This is of particular interest since the  $d$ -quark density at high  $x$  is poorly constrained by fixed-target experimental data with significant uncertainties from nuclear corrections which are not necessary at HERA. It can be seen that the data are well described by the Standard Model. The contribution from  $d$ -type quarks calculated using the H1 QCD fit is also

shown. At low  $Q^2$  and low  $x$  it can be seen that the measurements are sensitive to the sea quark distributions.

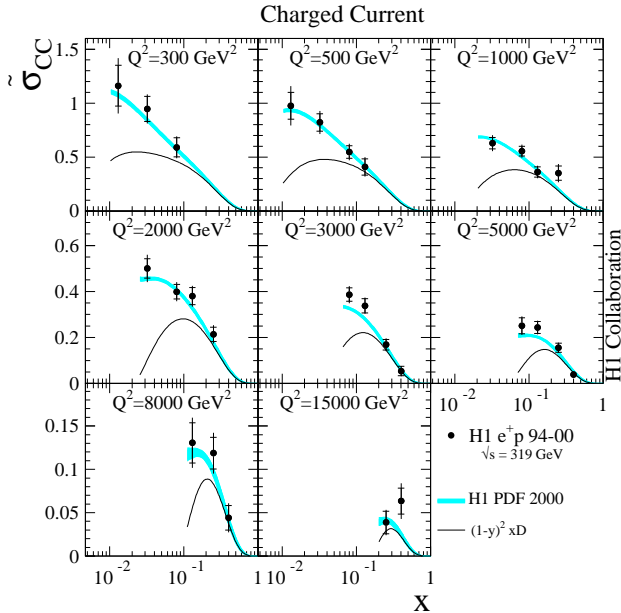


Fig. 6: The reduced cross section for CC DIS from the H1 collaboration.

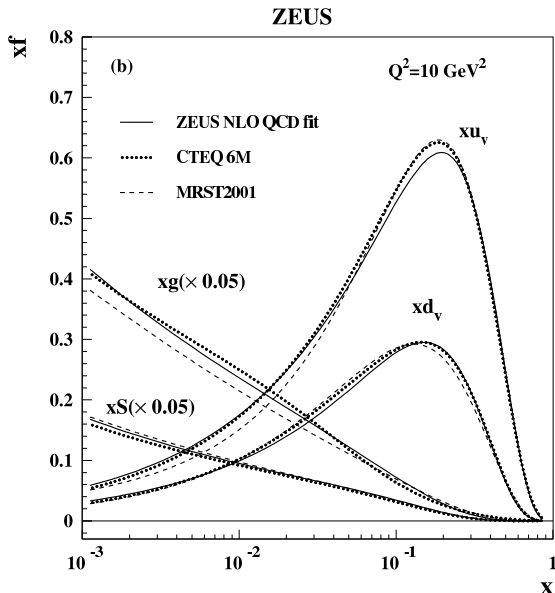


Fig. 7: Parton distribution functions extracted from the ZEUS NLO QCD fit.

Figure 7 shows the gluon, sea and valence parton distribution functions extracted from the ZEUS NLO QCD fit at  $Q^2 = 100 \text{ GeV}^2$  as a function of  $x$ . Also shown

are the corresponding PDFs from the CTEQ6 [16] and MRST(2001) [12] fits. Differences between the predictions in the valence quark and gluon distributions reflect differences in the parameterisations used, data sets included and other assumptions made in the analyses, however generally the fits give a consistent picture of the proton PDFs.

## 7. Summary and future prospects

Cross sections for neutral and charged current deep inelastic scattering interactions have been presented by the H1 and ZEUS collaborations. In all cases the Standard Model gives a good description of the data. The proton structure functions have been extracted from the measured cross sections. Measurements of  $F_2$  by the ZEUS and H1 collaborations over a large range in  $x$  and  $Q^2$  are in excellent agreement with each other and the Standard Model. Values of the longitudinal structure function  $F_L$  are starting to give direct information on the gluon density in the proton and measurements of  $xF_3$  confirm the valence structure of the proton at high  $Q^2$ .

The goal of the HERA upgrade is to provide integrated luminosities of  $1 \text{ fb}^{-1}$  to the H1 and ZEUS experiments. The precision of NC and CC DIS cross section measurements at high  $Q^2$  will benefit from the increase in luminosity that the HERA upgrade will provide. In particular determination of the  $u$  and  $d$  quark densities at high  $Q^2$  and at high  $x$  will be possible with much improved accuracy. The introduction of longitudinally polarised lepton beams for the H1 and ZEUS experiments will allow the investigation of the chiral nature of the Standard Model in  $ep$  scattering. Searches for right-handed charged currents and the determination of the vector and axial-vector couplings of the  $Z^0$  to the  $u$  and  $d$  quarks will be among the measurements possible at high  $Q^2$  with high luminosity and longitudinally polarised lepton beams.

## Acknowledgments

I would like to thank the organisers for a very interesting conference and the Imperial College London HEP group for the opportunity to attend the conference.

1. ZEUS Collab., U. Holm (ed.), *The ZEUS Detector*, Status Report (unpublished), DESY, 1993.
2. H1 Collab., I. Abt *et al.*, *Nucl. Instrum. Methods* **A36**, 310 (1997).
3. H1 Collab., Abstract 083, International Europhysics Conference on High Energy Physics, EPS03, July 17-23, 2003, Aachen.

4. ZEUS Collab., Abstract 502, International Europhysics Conference on High Energy Physics, EPS03, July 17-23, 2003, Aachen.
5. ZEUS Collab., S. Chekanov *et al.*, Phys. Rev. **D67**, 012007 (2002).
6. ZEUS Collab., J. Breitweg *et al.*, Eur. Phys. J. **C12** (2000) 3, 411.
7. R.S. Thorne and R.G. Roberts, Eur. Phys. J. **C19**, 339 (2001).
8. H1 Collab., C. Adloff *et al.*, Preprint DESY-03-038, Accepted by Eur. Phys. J.
9. H1 Collab., C. Adloff *et al.*, Eur. Phys. J. **C21** (2001) 33.
10. H1 Collab., Abstract 799, International Europhysics Conference on High Energy Physics, EPS01, July 12, 2001, Budapest.
11. H1 Collab., Abstract 082, International Europhysics Conference on High Energy Physics, EPS03, July 17-23, 2003, Aachen.
12. A. D. Martin *et al.*, Eur. Phys. J. **C23**, 73 (2002).
13. S. I. Alekhin, Phys. Rev. **D68**, 114002 (2003).
14. H1 Collab., C. Adloff *et al.*, Eur. Phys. J. **C19** (2001) 269.
15. ZEUS Collab., S. Chekanov *et al.*, Eur. Phys. J. **C28** (2002) 2, 175.
16. J. Pumplin *et al.*, JHEP 07, 012 (2002).